Journal of Alloys and Compounds 499 (2010) 154–159

Contents lists available at ScienceDirect

Journal of Alloys and Compounds

journal homepage: www.elsevier.com/locate/jallcom

Effects of cerium content on wettability, microstructure and mechanical properties of Sn–Ag–Ce solder alloys

Bo-In Noh, Jung-Hyun Choi, Jeong-Won Yoon, Seung-Boo Jung*

School of Advanced Materials Science and Engineering, Sungkyunkwan University, 300 Cheoncheon-dong, Jangan-gu, Suwon, Gyeonggi-do 440-746, Republic of Korea

ARTICLE INFO

Article history:
Received 30 September 2009
Received in revised form 19 March 2010
Accepted 19 March 2010
Available online 25 March 2010

Keywords:
Pb-free solder
Rare earth element
Wettability
Microstructure
Hardness
Tensile strength

ABSTRACT

We investigated the effects of adding small amounts of cerium (Ce) to low Ag content Sn solder (Sn–1.0 wt.%Ag) on melting temperature, microstructure, wettability and mechanical properties using differential scanning calorimeter, optical microscope, scanning electron microscope, energy dispersive X-ray spectroscopy, wetting balance tester, Vickers hardness tester and tensile tester assays. The addition of Ce had little influence on the melting behavior of Sn–1.0Ag solder, but improved its wettability, mechanical properties, and microstructure.

1. Introduction

Concern about the environment is leading to increased regulatory and consumer pressure on the electronics industry to reduce or eliminate the use of lead (Pb) in product manufacture [1]. Currently several Pb-free solder alloys, such as Sn–Ag, Sn–Cu, Sn–In, Sn–Bi, Sn–Zn, Sn–Ag–Cu, and Sn–Zn–Bi, have been developed for use in practical applications. Among these, Sn–Ag and Sn–Ag–Cu solders are the leading candidates to replace Pb-containing solders because of their good comprehensive properties [2]. However, some problems with Sn–Ag or Sn–Ag–Cu solders remain, such as the formation of large brittle intermetallic compounds (IMCs) and short creep-rupture lifetime in service [3,4]. To meet the demand for increasingly finer pitch and durability under severe service conditions, novel Pb-free solders with better creep and thermal fatigue performances are required. It has been proposed that the addition of a third or fourth element to the alloy would further improve the performance of Sn–Ag or Sn–Ag–Cu solders [5].

In recent years, many attempts have been made to add rare earth (RE) elements to Pb-free solder alloys to improve their microstructures, mechanical properties and wettabilities. RE elements have been called the "vitamins of metals," in that minute quantities may greatly enhance the properties of metals or alloys [3,6–15]. RE elements are surface-active elements, which play an important role in metallurgy, participating in the refinement of microstructure, alloys, purification of materials and metamorphosis of inclusions [6]. There are two types of RE elements. One is made up of the light RE or Ce group of elements that includes La, Ce, Pr, Nd, Pm, Sm, and Eu. The other group includes the heavy RE or Y group of elements, such as Er, Y, Sc, Gd, Tb, and Yb. Recent studies on the effects of RE elements in Pb-free solders generally included light RE elements, such as La, Ce, or a mixture of both [7,8]. Chen et al. reported that the addition of a minute amount of RE was an effective way to improve the high temperature performance of solder alloy [9–11]. Wu et al. observed that small additions of RE elements into a Sn–9Zn system improved wettability and tensile strength [12,13]. It was reported that the addition of RE elements had little influence on melting behavior of Sn–3.8Ag–0.7Cu solders, but the solder showed better wettability and mechanical properties, as well as finer microstructures [14]. With the addition of RE elements, the thickness of the IMC layer at the solder/Cu interface decreased during soldering and the growth of IMCs was constrained after high temperature aging [15].

Recently, the electronics manufacturing field has been interested in Pb-free solders with low Ag content due to the cost efficiency and superior drop reliability of the solder alloy [16–18]. Therefore, in this study, the effects of small additions of Ce to low Ag solder (Sn–1.0 wt.%Ag solder) on melting temperature, microstructure, wettability and mechanical properties were investigated.

* Corresponding author. Tel.: +82 31 290 7359; fax: +82 31 290 7371.
E-mail addresses: nohbi@skku.edu (B.-I. Noh), jwy4918@skku.edu (J.-W. Yoon), sbjung@skku.ac.kr (S.-B. Jung).

0925-8388/$ – see front matter © 2010 Elsevier B.V. All rights reserved.
doi:10.1016/j.jallcom.2010.03.179

Table 1
Conditions of the wetting balance test.

Cu specimen size	7.0 mm × 30.0 mm × 0.2 mm
Atmosphere	Air
Immersion time	10 s
Immersion depth	5 mm
Immersion speed	10 mm/s

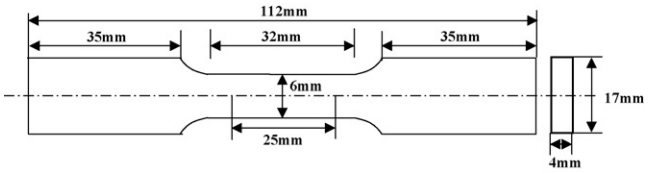

Fig. 1. Schematic presentation of the tensile test specimen.

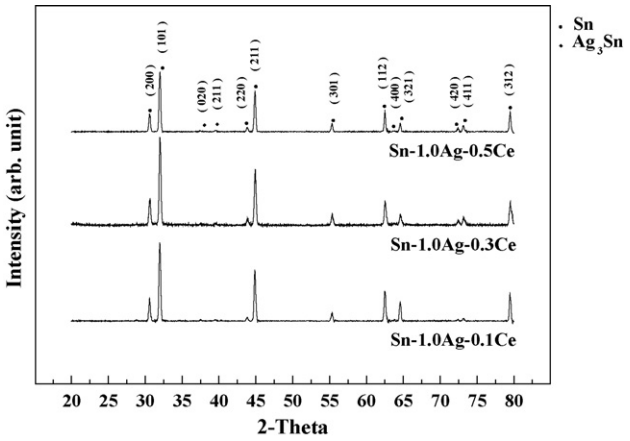

Fig. 3. XRD patterns for the Sn–1.0Ag–*x*Ce solders.

2. Experimental procedures

2.1. Solder alloy design and preparation

Pure Sn, Ag and Ce metals with purities of 99.99, 99.99 and 99.0 (in wt.%), respectively, were used as raw materials. Three alloys, Sn–1.0Ag–0.1Ce, Sn–1.0Ag–0.3Ce and Sn–1.0Ag–0.5Ce (in wt.%), were manufactured. The pure metals were mixed and melted in a graphite reactor at 600 °C for 30 min in an argon gas atmosphere. The power of the induction furnace and gas pressure was 9 kW and 500 Torr, respectively.

After manufacturing of the solder alloy, inductively coupled plasma-optical emission spectrometer (ICP-OES) analysis was performed for the three parts of each solder alloy to identify the composition.

2.2. Melting temperature of the solder alloys

The melting temperatures of the solder alloys were measured with a differential scanning calorimeter (DSC). Approximately 10 mg of solder was placed into an aluminum cell for DSC analysis. The scanning temperature range was set from 25 to 300 °C at a heating and cooling rate of 10 °C/min under nitrogen atmosphere.

2.3. XRD analysis

To analysis phases of the solder alloys, X-ray diffraction (XRD) analysis was performed. The XRD patterns were recorded at room temperature using a Rigaku (Japan) diffractometer. The filament voltage and current were set to 30 kV and

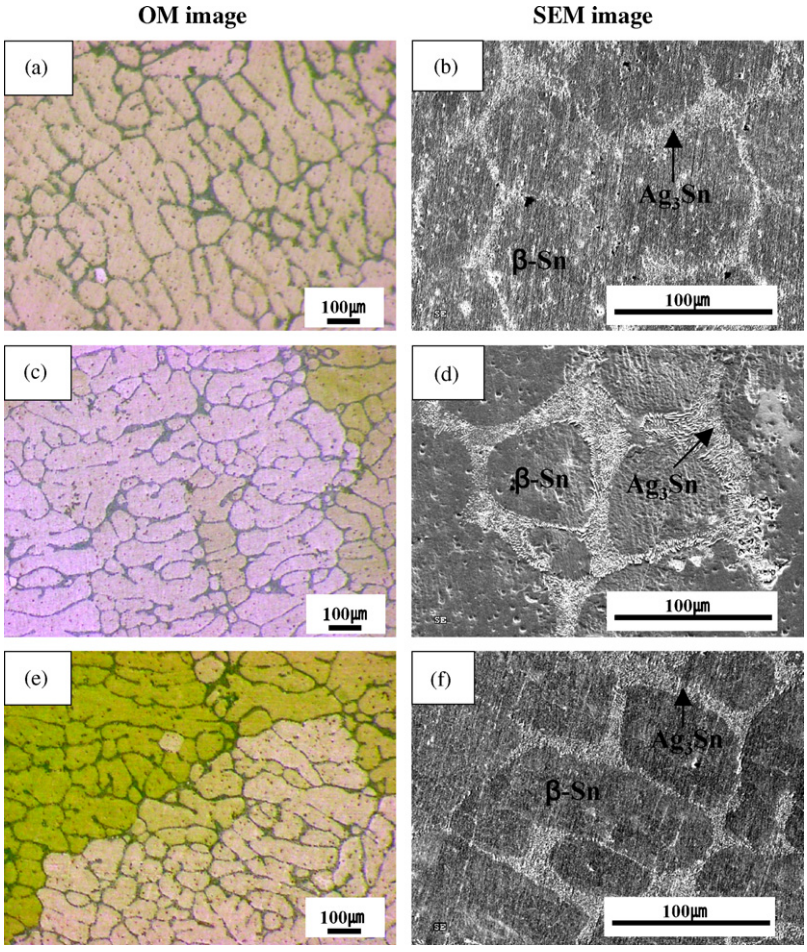

Fig. 2. OM and SEM images of the Sn–1.0Ag–*x*Ce solder alloys: (a, b) Sn–1.0Ag–0.1Ce, (c, d) Sn–1.0Ag–0.3Ce and (e, f) Sn–1.0Ag–0.5Ce.

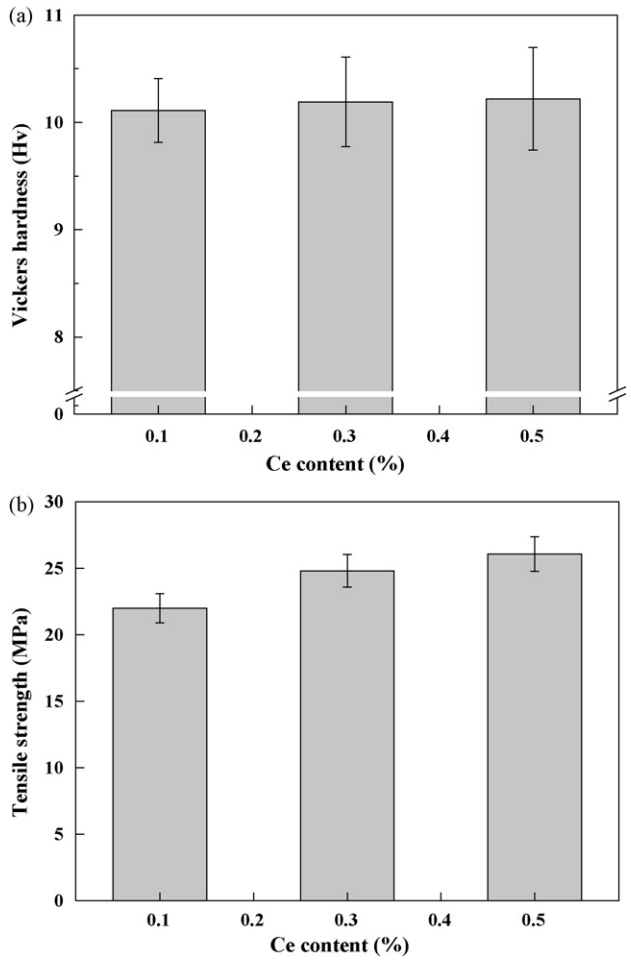

Fig. 4. Mechanical properties for the various solder alloys: (a) Vickers hardness and (b) tensile strength.

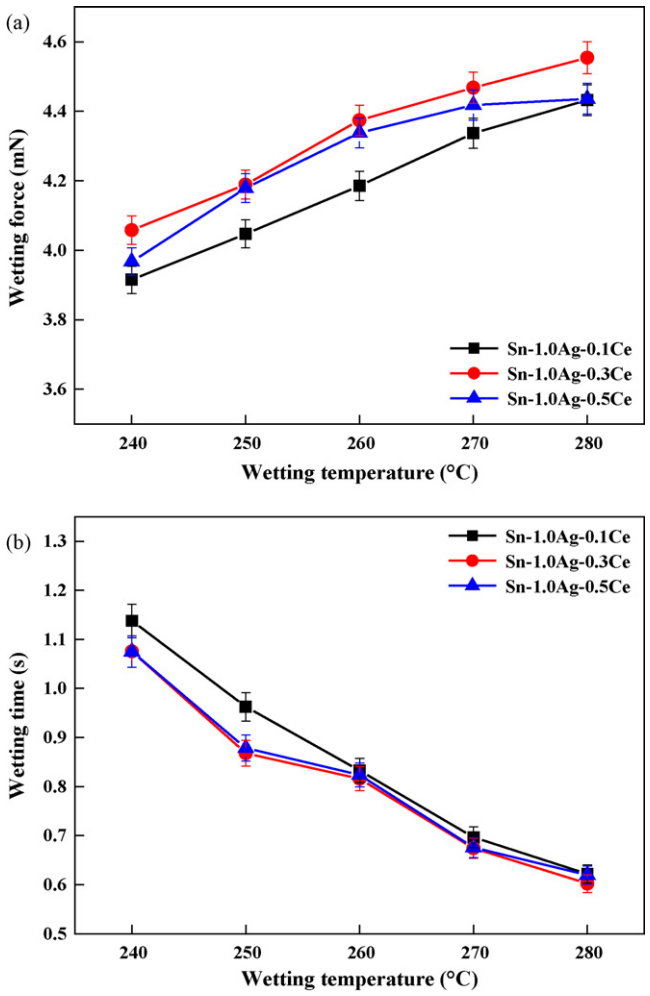

Fig. 5. Comparison of wettability for Sn–1.0Ag–*x*Ce solder alloys: (a) wetting force and (b) wetting time.

100 mA, respectively. The sample was scanned between 20° and 80° at a rate of 4°/min.

2.4. Wettability

The solderability of the solder alloys on a Cu substrate was measured by a wetting balance tester (SAT-5100, Rhesca Co. Ltd., Japan). This system is widely used for controlling the soldering process and assessing and improving soldering performance as it provides an assessing function developed on the basis meniscography (MIL-STD-883D) as a standard accessory. Cu coupons (7 mm × 30 mm × 0.2 mm) were etched in a 10% H_2SO_4 + 90% CH_3OH solution to remove surface oxides and contaminations. Prior to the test, each Cu coupon was dipped in rosin mildly activated (RMA)-type flux. Table 1 summarizes the conditions of the wetting balance test used in this study. The wetting temperature range was 240–280 °C. The same measurement conditions were used for all samples for a reliable comparison of their solderabilities. Ten measurements were made for each condition. The common attributes in the wetting force measurements, maximum wetting force (F_{max}) and zero crossing time (T_{zero}), were used to assess the wetting behavior of the solder alloys.

2.5. Microstructure

The microstructures of the solder alloys and IMCs formed at the interface between the solder and substrates in the wetting test were investigated by optical microscopy (OM), scanning electron microscopy (SEM, S-3000H, Hitachi, Japan) and energy dispersive X-ray spectroscopy (EDS). The common metallographic practices of grinding and polishing were used to prepare the samples. An etchant consisting of 95% C_2H_5OH–4% HNO_3–1% HCl was used to reveal the cross-sectional microstructure.

2.6. Mechanical properties

The hardness and tensile strength of the solder alloys were investigated by Vickers hardness and tensile tests, respectively. The loading condition of the hardness test and tensile speed were 200 gf and 2 mm/min, respectively. Fig. 1 shows the schematic presentation of the tensile test specimen.

3. Results and discussion

Melting temperature is a crucial physical property and is important influence on the quality of solder alloys. In this study, melting temperatures were evaluated by DSC measurement of enthalpy variation during the melting process. The onset point of the DSC heating curve is related to the solidus temperature and the peak point is recognized as the liquidus temperature of solder alloys [19]. Additionally, undercooling is defined as the temperature difference between the melting temperature of a solder alloy during heating and the solidification temperature during cooling. One of the distinct properties of Sn-rich solders is a propensity for a large amount of undercooling of the β-Sn phase during solidification. Since the undercooling phenomenon is related to the difficulty of nucleating a solid phase in a liquid state, it can be influenced by many metallurgical parameters, such as solder composition, solder volume, and impurity level. It was reported that the addition of minor alloying elements, such as Zn, Fe, Co, Ni, Bi and others could reduce the amount of undercooling of β-Sn [20,21]. In addition, the large undercooling can also affect the microstructures of Sn-rich solder alloys as well as their mechanical properties.

Table 2 shows the results of DSC analysis for various solder alloys. For each solder, the onset and peak temperatures of the DSC curve were recorded. The onset temperature of the solder alloys

Table 2
DSC results for the solder alloys.

Solder	Heating		Cooling		Undercooling (°C)
	Onset temp. (°C)	Peak temp. (°C)	Onset temp. (°C)	Peak temp. (°C)	
Sn–1.0Ag–0.1Ce	217.5	230.0	226.1	223.1	3.9
Sn–1.0Ag–0.3Ce	218.1	230.6	225.1	222.7	5.5
Sn–1.0Ag–0.5Ce	218.5	230.8	223.7	222.4	7.1

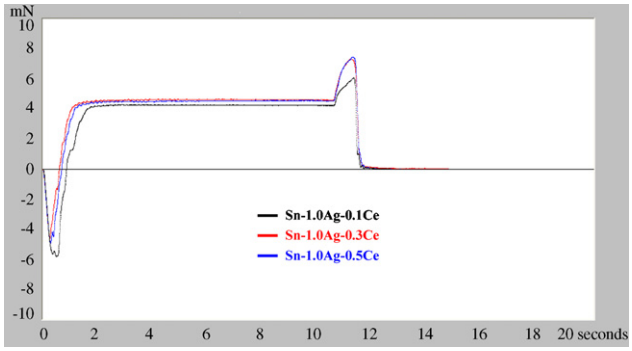

Fig. 6. Wetting curves of the Sn–1.0Ag–*x*Ce solder alloys (wetting temperature: 250 °C).

increased slightly from 217.5 to 218.5 °C with increasing Ce during heating, while the onset temperature decreased from 226.1 to 223.7 °C during cooling. The peak temperature of the heating reaction increased slightly from 230 to 230.8 °C with increasing Ce, while the peak temperature of the cooling reaction decreased from 223.1 to 222.4 °C. From these results, the temperature in the heating reaction was seen to increase slightly with increasing Ce, while the temperature in the cooling reaction was slightly decreased. Additionally, the undercooling increased from 3.9 to 7.1 °C with increasing Ce in the Sn–1.0Ag–*x*Ce solder alloy. Although a small addition of Ce to the Sn–1.0Ag solder slightly increased the melting temperature, this change was not significant. Thus, the use of Sn–Ag solder containing a small amount of Ce did not alter the heating conditions in the reflow processing of the Sn–Ag solder.

Fig. 2 shows the microstructures of solder alloys with different Ce content. Ce was observed to affect the microstructure of solder alloy. The microstructure of the Sn–1.0Ag–*x*Ce solder alloys consisted of β-Sn and Ag_3Sn phases, and the microstructure became finer with greater Ce content. Zhao et al. also reported that the microstructure of Sn–Ag–Cu solders became finer and the distribution was more homogenous as the content of Ce increased [22]. Xia reported that a small amount of Ce was absorbed by the boundaries of IMCs and provided an inhomogeneous center of nucleation that changed the crystal growth velocities along with various crystalline directions [23]. From these results, we anticipated that the microstructural change would affect the mechanical properties of the solder alloy.

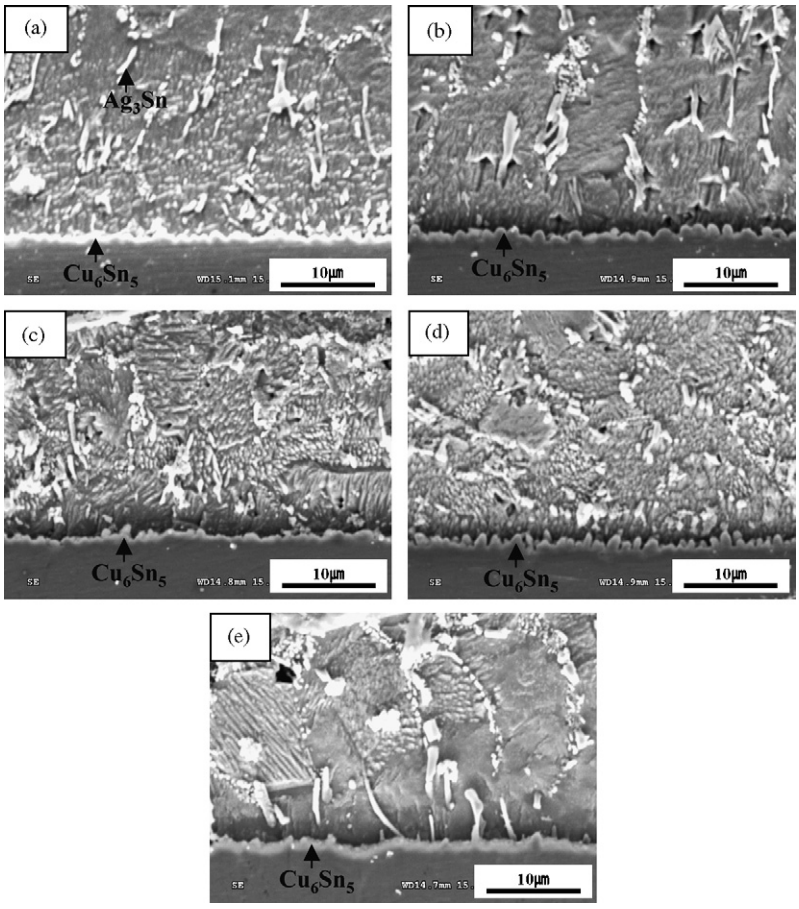

Fig. 7. Cross-sectional SEM images of the Sn–1.0Ag–0.3Ce solder alloys after wetting at (a) 240, (b) 250, (c) 260, (d) 270 and (e) 280 °C.

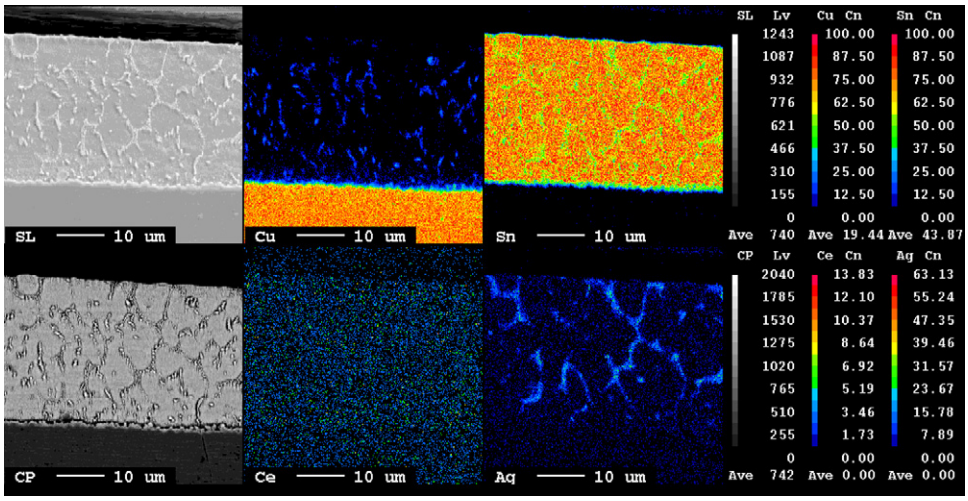

Fig. 8. EPMA mapping analysis result of the Sn–1.0Ag–0.5Ce/Cu joint.

The XRD patterns of the solder alloys are shown in Fig. 3. The XRD patterns revealed that the Sn–1.0Ag–*x*Ce solders were consisted of β-Sn and Ag_3Sn phases. XRD analysis confirmed that no Ce-containing phase or Ce element was detected in the solder matrix. When comparing the three kinds of solder joints, no significant difference was observed.

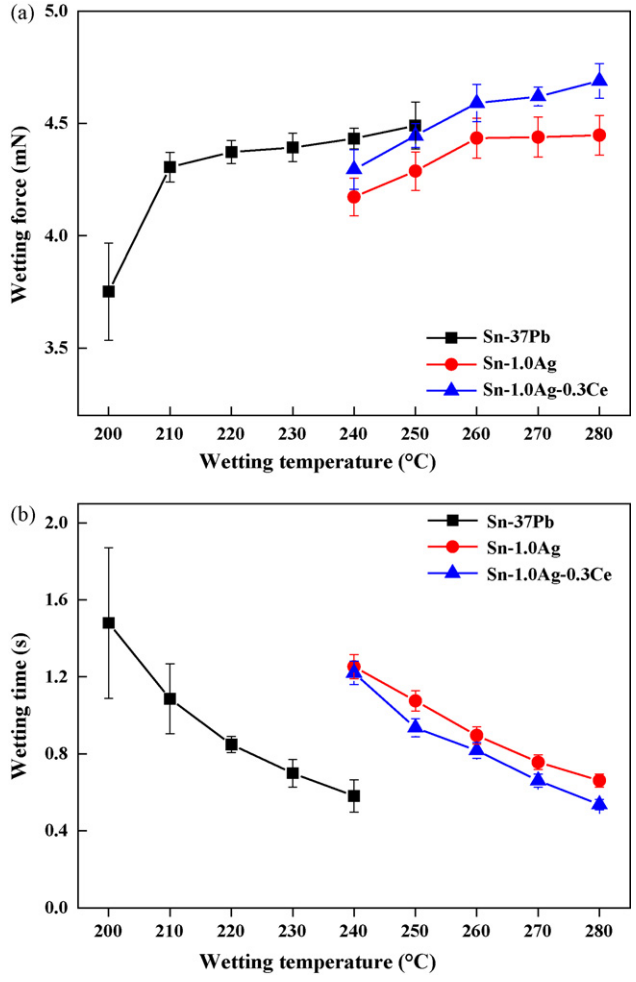

Fig. 9. Comparison of wettability for various solder alloys: (a) wetting force and (b) wetting time.

Fig. 4 shows the results of mechanical tests for various solder alloys. The Vickers hardness of the Sn–1.0Ag–*x*Ce solders was nearly the same (or slightly increased), however, the tensile strength of the solder alloy increased with increasing Ce content. The Vickers hardness values of the Sn–1.0Ag–*x*Ce solders with 0.1 wt.% Ce, 0.3 wt.% Ce, and 0.5 wt.% Ce were 10.11, 10.19, and 10.22 Hv, respectively. On the other hand, the values of the tensile strength of the Sn–1.0Ag–*x*Ce solders with 0.1 wt.% Ce, 0.3 wt.% Ce, and 0.5 wt.% Ce were 21.99, 24.81, and 26.08 MPa, respectively. These results were affected by the finer microstructures obtained with higher Ce content. RE elements tend to be absorbed at the grain boundary and decrease boundary movement. In addition, the strain field of large RE atoms and dislocations interact and restrain the movement of dislocations, thus increasing the tensile strength of a solder joint [3]. Therefore, the mechanical properties of the Sn–Ag–Ce alloys were improved by the addition of 0.1–0.5 wt.% Ce to the Sn–1.0Ag solder alloy.

Fig. 5 shows the results of wetting tests for the Sn–1.0Ag–*x*Ce solder alloys. The wetting force increased with increasing wetting temperature, while the wetting time decreased, irrespective of the kind of solder alloy. We anticipated that the high wetting temperature decreased the surface tension between the molten solder and substrate or between the molten solder and flux, and therefore the wettability was improved. The wetting force of the Sn–1.0Ag–*x*Ce solder alloys increased up to 0.3 wt.% Ce, and decreased above 0.3 wt.% Ce. In contrast, the wetting time of the Sn–1.0Ag–*x*Ce solder alloys decreased up to 0.3 wt.% Ce, and slightly increased above 0.3 wt.% Ce. Fig. 6 shows the wetting curves of the Sn–1.0Ag–*x*Ce solder alloys at 250 °C. In comparing the 0.1–0.5 wt.% Ce, the wetting force and wetting time of the solder alloy with 0.5 wt.% Ce were greater and shorter than that with 0.1 wt.% Ce, respectively. Generally, RE is a surface-active element, which can decrease the surface tension of liquid solder and enhance the wetting of a substrate. However, RE is liable to oxidation [24]. The formation of an oxide residue during soldering may deteriorate the wettability of the solder. As a result, the disadvantages of the oxide residue may exceed the favorable aspects. Therefore, it is suggested that the appropriate range of Ce should be 0.3 wt.% for optimum wettability with high wetting force and short wetting time of the Sn–1.0Ag–*x*Ce solder alloy.

Fig. 7 shows the cross-sectional SEM images of the Sn–1.0Ag–0.3Ce/Cu interfaces after wetting tests at different temperatures. The solder/substrate interfaces were very uniform, a Cu_6Sn_5 IMC formed at the interface between the solder and Cu substrate, and the Ag_3Sn phases are evenly distributed in the

solder region. EPMA mapping analysis was performed and the corresponding result was shown in Fig. 8. The highest Ce-containing Sn–1.0Ag–0.5Ce solder was used in the EMPA analysis to investigate the behavior of Ce element. The EPMA mapping result revealed that the solder matrix was composed of the β-Sn, Cu_6Sn_5, and Ag_3Sn. In addition, the Ce elements are evenly distributed in the solder region and no Ce-containing IMCs were detected in the solder matrix.

Fig. 9 shows the comparison results of wettability for various solder alloys. The flux was different from that used in Fig. 5. Compared to the Sn–1.0Ag solder alloy, the wetting force of the Sn–1.0Ag–0.3Ce solder alloy was greater, while the wetting time was shorter, suggesting that the addition of 0.3 wt.% Ce improved the wettability of the Sn–1.0Ag solder alloy. Although the wetting temperature ranges of the Sn–37Pb and Sn–1.0Ag–0.3Ce solder alloys are different due to their different melting temperatures, the wetting force of the Sn–1.0Ag–0.3Ce solder was greater, while the wetting time for the two solder alloys was similar. To this end, the Sn–1.0Ag–0.3Ce solder alloy can replace the conventional Sn–37Pb or Sn–1Ag solder alloy because of the superior wettability and mechanical properties of the solder.

4. Conclusions

We investigated the effects of small additions of Ce to low Ag containing Sn–1.0 wt.%Ag solder on melting temperature, microstructure, wettability and mechanical properties. Although the addition of a small amount of Ce to Sn–1.0Ag solder slightly increased its melting temperature, there was no significant change in the melting temperature of the solder alloys. The microstructure of the Sn–1.0Ag–*x*Ce solder alloys became finer with increasing Ce. In the mechanical tests, the Vickers hardness of the Sn–1.0Ag–*x*Ce solders was nearly the same, however, the tensile strength of the solder alloy increased with increasing Ce. The wettability increased in the following order: Sn–1.0Ag–0.3Ce, Sn–1.0Ag–0.5Ce and Sn–1.0Ag–0.1Ce. In conclusion, the addition of Ce had little influence on melting behavior, however, the resulting solder alloy showed better wettability and mechanical properties. Therefore, Sn–1.0Ag–0.3Ce solder alloy may be a suitable substitute for conventional Sn–37Pb or Sn–1Ag solder alloy because of its superior wettability and mechanical properties.

Acknowledgement

This work was supported by the Component Material Technology Development Program of the Ministry of Commerce, Industry, and Energy (MOCIE).

References

[1] B. Vandevelde, M. Gonzalez, P. Limaye, P. Ratchev, E. Beyne, Microelectron. Reliab. 47 (2007) 259–265.
[2] M. Abtew, G. Selvaduary, J. Mater. Sci. Eng. R 27 (2000) 95–141.
[3] C.M.L. Wu, D.Q. Yu, C.M.T. Law, L. Wang, Mater. Sci. Eng. R 44 (2004) 1–44.
[4] K.S. Kim, S.H. Huh, K. Suganuma, J. Alloys Compd. 352 (2003) 226–236.
[5] K.S. Kim, S.H. Huh, K. Suganuma, Microelectron. Reliab. 43 (2003) 259–267.
[6] Y.W. Shi, J. Tian, H. Hao, Z.D. Xai, Y.P. Lei, F. Guo, J. Alloys Compd. 453 (2008) 180–184.
[7] B. Li, Y.W. Shi, Y.P. Lei, F. Guo, Z.D. Xia, B. Zong, J. Electron. Mater. 34 (2005) 217–224.
[8] D.Q. Yu, J. Zhao, L. Wang, J. Alloys Compd. 376 (2004) 170–175.
[9] Z.G. Chen, Y.W. Shi, Z.D. Xia, Y.F. Yan, J. Electron. Mater. 31 (2002) 1122–1128.
[10] Z.G. Chen, Y.W. Shi, Z.D. Xia, Y.F. Yan, J. Electron. Mater. 32 (2003) 243–245.
[11] Z.G. Chen, Y.W. Shi, Z.D. Xia, Y.F. Yan, J. Electron. Mater. 33 (2004) 964–971.
[12] C.M.L. Wu, D.Q. Yu, C.M.T. Law, L. Wang, J. Electron. Mater. 31 (2002) 921–927.
[13] C.M.L. Wu, D.Q. Yu, C.M.T. Law, L. Wang, J. Electron. Mater. 32 (2003) 63–69.
[14] H. Hao, J. Tian, Y.W. Shi, Y.P. Lei, Z.D. Xia, Y. Rare, Met. Mater. Eng. 35 (2006) 121–123.
[15] H. Hao, J. Tian, Y.W. Shi, Y.P. Lei, Z.D. Xia, J. Electron. Mater. 36 (2007) 766–774.
[16] Y.S. Lai, P.F. Yang, C.L. Yeh, Microelectron. Reliab. 46 (2006) 645–650.
[17] F. Sun, P. Hochstenbach, W.D. Van Driel, G.Q. Zhang, Microelectron. Reliab. 48 (2008) 1167–1170.
[18] H.C. Kim, M. Zhang, C.M. Kumar, D.W. Suh, P. Liu, D.W. Kim, M. Xie, Z. Wang, 57th Electron. Comp. Technol. Conf. (2007) 962–967.
[19] L. Zhang, S.B. Xue, L.L. Gao, G. Zeng, Z. Sheng, Y. Chen, S.L. Yu, J. Mater. Sci: Mater. Electron. 20 (2009) 685–694.
[20] I.E. Anderson, J.L. Harringa, J. Electron. Mater. 35 (2006) 94–106.
[21] S.K. Kang, D. Leonard, D.Y. Shih, L. Gignac, D.W. Henderson, S. Cho, J. Yu, J. Electron. Mater. 35 (2006) 479–485.
[22] X.Y. Zhao, M.Q. Mai, X.Q. Cui, T.H. Xu, M.X. Tong, Trans. Nonferrous Met. Soc. China 17 (2007) 805–810.
[23] Z.D. Xia, J. Mater. Sci. 31 (2002) 564–569.
[24] L. Wang, D.Q. Yu, J. Zhao, M.L. Huang, Mater. Lett. 56 (2002) 1039–1042.